Predicting the gas/particle distribution of SVOCs in the indoor environment using poly-parameter Linear Free Energy Relationships

Tunga Salthammer [1) *], Kai-Uwe Goss [2)]

[1)] Fraunhofer WKI, Department of Material Analysis and Indoor Chemistry, Bienroder Weg 54E, 38108 Braunschweig, Germany

[2)] Department Analytical Environmental Chemistry, Helmholtz-Centre for Environmental Research - UFZ , Permoserstraße 15, 04318 Leipzig, Germany

[*)] Author for Correspondence

Prof. Dr. Tunga Salthammer

Phone:+49-531-2155-213

Email tunga.salthammer@wki.fraunhofer.de

Keywords

Indoor SVOCs, gas/particle partitioning, hexadecane/air partitioning, descriptors, Linear Free Energy Relationships

Abstract

Understanding the partitioning of semi volatile organic compounds (SVOCs) between gas phase and particle phase is essential for exposure analysis and risk assessment in the indoor environment. Numerous attempts have been made to calculate gas/particle partitioning coefficients K_{ip}. Single-parameter adsorption and absorption models, which relate K_{ip} to the vapor pressure P_s or the octanol/air distribution coefficient K_{OA} are usually applied. In this work we use poly-parameter Linear Free Energy Relationships (pp-LFER) to describe the partitioning behavior of 14 SVOCs with high relevance for the indoor environment. The pp-LFER concept is based on Abraham descriptors and considers interactions between molecule and particle by separate parameters. Van der Waals interactions can be approximated by the logarithm of the hexadecane/air partitioning coefficient (log K_{HdA} = L), which is a key parameter for the 14 polar but non-ionizable organic esters being studied here. For many of the examined compounds experimentally determined L-values were not available and had to be measured using gas chromatography. It is shown that the pp-LFER method is a strong alternative to one-parameter approaches and gives reliable coefficients for gas/particle distribution in the indoor environment.

Graphical Abstract

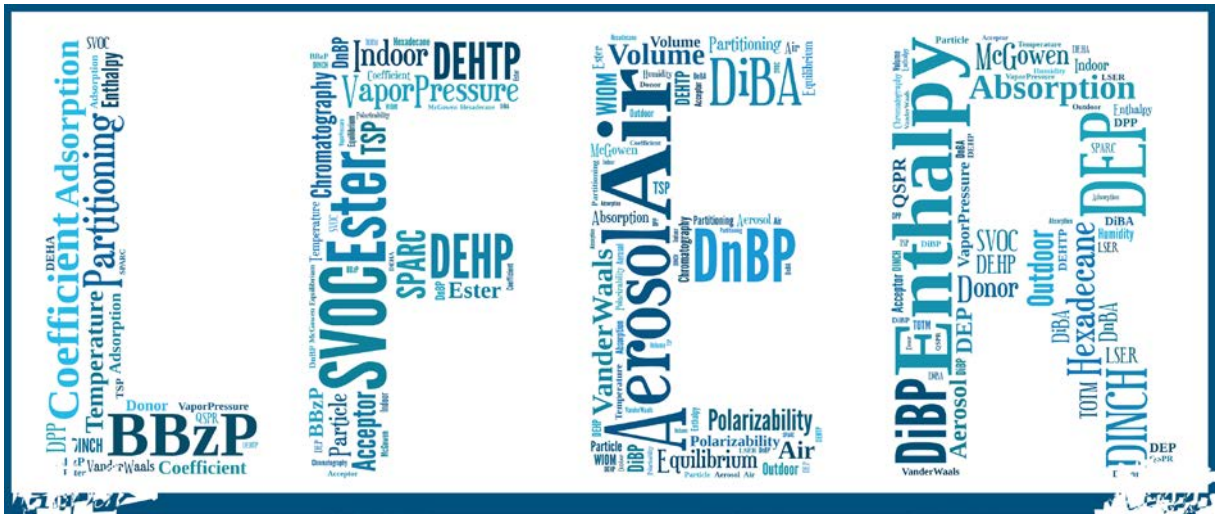

1. Introduction

The indoor area represents a multiple dynamic system comprised of emission sources and sinks.[1, 2] Describing the behavior of molecules and their interaction with the various compartments in dependence of temperature, relative humidity and air exchange rate is therefore correspondingly complex.[3] Then again, for exposure analysis, it is necessary to at least be able to estimate the equilibrium distribution of airborne indoor-relevant organic compounds between gas and particle phase.[4] In other words, a comprehensive risk assessment requires the information to what percentage a substance enters the lung via gas phase and particle phase, respectively.

A first adsorption-based model was developed by Junge for the global transport of persistent compounds in outdoor air.[5, 6] Pankow[7, 8] subsequently expanded Junge's approach to include the mechanism of absorption. The saturation vapor pressure (P_s) of the respective observed substance is required by both models as a central molecular parameter.

$$\log K_{ip} = m \cdot \log P_s + b \quad (1)$$

In equation (1), K_{ip} denotes the partition coefficient between gas phase and particle phase, whilst *m* and *b* represent the slope and the axis intercept of the linear equation. For substances which are solid in the observed temperature range, the vapor pressure of the subcooled liquid P_L^0 is used instead of P_s. Finizio et al.[9] interpret K_{ip} as the interaction between air and the organic phase of a particle. Accordingly, in equation (2), K_{ip} is linked to the octanol/air partition coefficient (K_{OA}) and the organic proportion of the particle f_{om}.

$$\log K_{ip} = \log K_{OA} + \log f_{OM} - 11.91 \quad (2)$$

Via equation (3), K_{ip} is also experimentally accessible.[8, 10]

$$K_{ip} = \frac{[F]/[TSP]}{[A]} = \frac{C_p}{C_g} \quad (3)$$

[TSP] (µg/m³) is the concentration of total suspended particulate matter, *[F]* (ng/m³) and *[A]* (ng/m³) are the particle and gas phase concentrations of the target compound, respectively. *[F]/[TSP]* = C_p (ng/µg) is the concentration in/on the particle phase per µg *TSP* and and C_g = *[A].*[11]

Rearrangement of equation (3) leads to equation (4), which defines the fraction (Φ) of a compound *i* in the particle phase.

$$\Phi = \frac{[F]}{[F]+[A]} = \frac{K_{ip} \cdot [TSP]}{1+K_{ip} \cdot [TSP]} \quad (4)$$

The theoretical derivations for the determination of K_{ip} were critically analyzed by Goss and Schwarzenbach.[12] In particular the fact that neither equation (1) nor equation (2) takes into

account the specific intermolecular interactions that govern every sorption process and that depend on the respective chemical structure of the molecules and the sorbing phase should be regarded as disadvantageous. Klöpffer[13] also considers this simplification to be a fundamental weakness in the model. Goss and Schwarzenbach[14] therefore proposed a more complex approach, the poly-parameter linear free energy relationship (pp-LFER), which is based on descriptors for the sorbing phase and the sorbing molecule in accordance with Abraham.[15] This approach considers the size of the compound, interaction abilities like van der Waals, H-accepting (e-donating) and H-donating (e-accepting) as well as a dipolarity/polarizability parameter, which describes polar interactions that are not covered by the other parameters. Van der Waals interactions can be approximated from the logarithm of the hexadecane/air partition coefficient $L = \log K_{HdA}$. The L term is experimentally accessible and contains an entropic contribution, which is of particular importance for systems where one of the phases is a gas.[16]

Various authors have applied equations (1) and (2) in order to determine the distribution of low-volatile organic compounds between gas and particle phase in indoor areas. Salthammer and Schripp,[17] however, demonstrated that the K_{ip} values calculated on the basis of P_s and K_{OA} can be riddled with substantial error for indoor scenarios. The pp-LFER[16] approach is a promising alternative and is applied for 14 indoor-relevant organic compounds. For a large number of these compounds, the logarithmic hexadecane/air partition coefficient L necessary as a descriptor was unknown and had to be determined initially. The results were compared with experimental and calculated K_{ip} values from single-parameter models and the suitability of the pp-LFER method for indoor applications was critically discussed. Aerosol descriptors were taken from Arp et al.,[18, 19] who studied gas/particle partitioning under consideration of ambient aerosol samples from different seasons and locations. Under the assumption that absorption into a water-insoluble organic matter (WIOM) phase is the dominating mechanism, the temperature dependence of the partitioning process can be described by the van't Hoff equation and the enthalpy for the distribution between air and WIOM. It was also necessary to evaluate the data set provided by Arp et al.[18, 19] for indoor applications. This was performed by a comparison with indoor aerosols for particle concentration, content of organic carbon and content of elemental carbon.

2. Theory of poly-parameter Linear Free Energy Relationships

2.1 Methodology of the LFER approach

The equilibrium constant K_{i_12} for partitioning of a given compound i between two phases 1 and 2 is connected to the free energy change of transfer $\Delta_{12}G_i$ via equation (5).

$$\ln K_{i\_12} = \frac{\Delta_{12}G_i}{R \cdot T} + \ln(const) \quad (5)$$

R is the universal gas constant and T is the temperature in K. Commonly, K_{i_12} is related to a known molecular property like the vapor pressure P_s or the octanol/air distribution coefficient K_{OA} in a linear double logarithmic correlation as shown in equations (1) and (2). This approach is known as single-parameter LFER. It is directly obvious that a single descriptor cannot account for the complete chemical diversity that arises from the various contributions of van der Waals and H-bond interactions. As outlined by Goss and Schwarzenbach,[14] the poly-parameter LFER approach uses a suite of 5 parameters in order to cover all relevant intermolecular interactions comprehensively. To this end, $\Delta_{12}G_i$ is divided into van der Waals- and a H-bond-components, which provides a more mechanistic understanding of the partition process. The interaction energies can then be estimated with the help of quantitative descriptors (see next section).

2.2 Linear Solvation Energy Relationship (LSER) descriptors

Goss[20] showed that the distribution of an organic compound between air and any condensed phase can be described with equation (6).

$$\log K_{ip}\,(m^3/g) = s \cdot S_i + a \cdot A_i + b \cdot B_i + l \cdot L_i + v \cdot V_i + c \quad (6)$$

S_i, A_i, B_i, L_i and V_i are compound-specific Abraham descriptors. S_i is the polarizability/dipolarizability), A_i is the hydrogen bond acidity (donor), B_i is the hydrogen bond basicity (acceptor), L_i is the logarithmic hexadecane/air partition coefficient log K_{HdA} (a surrogate for the van der Waals term) and V_i is the McGowan volume.[21] The sorbent-specific (here: particle-specific) parameters s, a, b, l and v describe the complementary sorbent properties. Together with the fitting constant c they can be determined at the given relative humidity (*RH*) by multiple-linear regression using experimental log K_{ip} values.

The McGowan volume V_i can be calculated from the molecular structure of the respective target compound following a procedure as described by Abraham and McGowan[21] (see also Table SI-1 in the Supporting Information). L_i can be determined experimentally by gas chromatography (see Sections 2.4 and 3.2). Another descriptor is the molar excess refractivity E_i, which is related to index of refraction and can be determined by a method as described by Abraham et al.[22] For many compounds E_i, S_i, A_i and B_i are available via the UFZ-LSER database.[23] For compounds with unknown descriptors, Quantitative Structure Property Relationships (QSPRs) have been developed for E, S, A, B and L. The QSPRs predict these LSER descriptors for chemicals based on structures provided as SMILES[24] (simplified molecular-input line-entry system) strings.[25, 26] For this work we saw the necessity to determine the L-values of our target chemicals experimentally although QSPR estimations

are available. The *L*-value is the single most influential molecular descriptor and therefore its accuracy is crucial for the overall result. Moreover, the expected *L*-values of our target compounds lie at the high end or even beyond the existing calibration data set of the QSPR method.

The pp-LFER approach can also be applied to predict the partition constant K_{isurf} for adsorption to a surface. K_{isurf} is defined by equation (7) as the concentration c_{surf} (µg/m²) of a compound *i* on the surface per unit surface area divided by c_g (µg/m³).

$$K_{isurf}\,(m) = \frac{c_{surf}}{c_g} \tag{7}$$

For adsorption to various surfaces at different relative humidity, K_{isurf} is a function of the van der Waals, donor and acceptor interactions as shown in equation (8).[27]

$$\log K_{isurf}\,(m) = a \cdot A_i + b \cdot B_i + l \cdot L_i + c \tag{8}$$

2.3 Determination of enthalpies

The absorptive partitioning between air and water-insoluble-organic-matter (WIOM) is given by the partitioning coefficient K_{p_wiom}. The temperature dependence of K_{p_wiom} can be described by the van't Hoff equation (9),

$$\ln K_{ip\_wiom} = -\frac{\Delta_{WIOM}H}{R} \cdot \frac{1}{T} + const \tag{9}$$

where $\Delta_{wiom}H$ is the enthalpy for the distribution between air and WIOM. Arp et al.[18] showed that $\Delta_{wiom}H$ can be approximated by the enthalpy of distribution between air and octanol $\Delta_{OA}H$ or by the enthalpy of vaporization $\Delta_{vap}H$. For octanol-air partitioning $\Delta_{OA}H$ values can be calculated from the pp-LFER approach according to equation (10).[16]

$$\Delta_{wiom}H \approx \Delta_{OA}H\,(kJ/mol) = +1.6 \cdot V_i - 9.7 \cdot L_i + 6.0 \cdot S_i - 53.7 \cdot A_i - 9.2 \cdot B_i - 6.7 \tag{10}$$

For a narrow temperature range the relationship between K_{p_wiom} values at temperatures T_1 and T_2 is given by equation (11).

$$\ln K_{ip\_wiom}(T_2) = \ln K_{ip\_wiom}(T_1) - \frac{\Delta_{wiom}H}{R} \cdot \left(\frac{1}{T_1} - \frac{1}{T_2}\right) \tag{11}$$

For the case of adsorption to a surface, Goss and Schwarzenbach[28] derived the empirical equation (12) to estimate the enthalpy of adsorption $\Delta_{surf}H_i$ from K_{isurf} at 288 K.

$$\Delta_{surf}H_i(kJ/mol) = -9.83 \cdot \log K_{isurf}\,(m) - 90.5 \tag{12}$$

Assuming that $\Delta_{surf}H_i$ is constant over a certain range of temperature, K_{isurf} at a temperature T can be estimated from published 288 K data.[29]

$$\ln K_{isurf}(T) = \ln K_{isurf}(288\ K) - \frac{\Delta_{surf}H_i\ (288\ K)}{R} \cdot \left(\frac{1}{T} - \frac{1}{288}\right) \quad (13)$$

2.4 Determination of hexadecane/air and octanol/air partitioning coefficients

According to Stenzel et al.,[30] the retention time of an organic substance is proportional to the stationary phase-gas partition coefficient in an isothermal gas chromatographic system with a suitable, completely non-polar column. Consequently, *L* can be experimentally determined from Equation (14).

$$\log(RT) = l_L \cdot L_i + v_L \cdot V_i + c_L \quad (14)$$

RT is the gas chromatographic retention time (min), the coefficients l_L, v_L und c_L can be determined through a calibration procedure.

K_{OA}-values can be estimated from the pp-LFER approach according to equation (15), descriptors for wet and dry octanol are presented in Table 3.

$$\log K_{OA} = e \cdot E_i + s \cdot S_i + a \cdot A_i + b \cdot B_i + l \cdot L_i + v \cdot V_i + c \quad (15)$$

3. Materials and methods

3.1 Compounds

All compounds are commercially available and were of analytical grade. Diethyl phthalate (DEP): Riedel-de-Haèn; di-n-butyl-phthalate (DnBP): Sigma-Aldrich; di-iso-butyl-phthalate (DiBP): Fluka; dipentyl phthalate (DPP): ABCR GmbH; butylbenzyl phthalate (BBzP): Follmann & Co. KG; di-2-ethylhexyl-phthalate (DEHP): Fluka; di-n-butyl adipate (DnBA): Sigma-Aldrich; di-iso-butyl adipate (DiBA): ABCR GmbH; di-2-ethylhexyl adipate (DEHA): Sigma-Aldrich; di-2-ethylhexyl terephthalate (DEHTP): Dr. Ehrenstorfer GmbH; tri-2-ethylhexyl trimellitate (TOTM): Fluka; tri-2-ethylhexyl phosphate (TEHP): Sigma-Aldrich; triphenyl phosphate (TPP): Sigma-Aldrich; 1,2-cyclohexane dicarboxylic acid diisononyl ester (DINCH): BASF (Hexamoll).

3.2 Analytical parameters and settings

GC/MS system: Hewlett-Packard 6890 GC with 5973 MSD; injector: Gerstel CAS3; injection volume: 0.2 µm; injector temperature: 110 °C to 330 °C (10 °C/s); inlet mode: split; split ratio: 60:1; column: Supelco SPB®-Octyl 30.0 m x 250 µm x 0.25 µm (280 °C max); constant flow; Helium flow: 0.6 ml/min; average velocity: 28 cm/s; oven program: isothermal; MSD mode: scan (m/z 35 – 800); solvent delay: 2.2 min.

For calibration we used three compounds with well-known *L*-values: DEP (*L* = 6.75)[30], DnBP (*L* = 8.59)[30] and DEHP (*L* = 12.70) for calibration.[31] V_i is the McGowan volume. All substances were analysed at 250 °C and 280 °C, respectively.

3.3 Determination of ompound-specific descriptors

S, *A*, *B*, *V* and *L* are listed in Table 1. The *L*-values were measured (see above) and the *V*-values were calculated (see Supporting Information). In case of DEP, DiBP, DPP, BBzP, DEHP, DnBA and TPP experimental descriptors are available for *S*, *A* and *B*. These were taken from the UFZ-LSER database.[23] For DiBA, DEHA, DEHTP, TOTM, TEHP and DINCH *S*, *A* and *B* were calculated from a QSPR approach.[23] The enthalpies for the distribution between air and WIOM $\Delta_{wiom}H$ were approximated from the enthalpies of vaporization $\Delta_{vap}H$[32-34] for DEP, DnBP, DiBP, DPP, BBzP and DEHP. For all other compounds $\Delta_{wiom}H$ was approximated from $\Delta_{OA}H$ according to equation (10).

Table 1: Abraham descriptors and enthalpies for the distribution between air and WIOM of the 14 compounds. The data from Rohac et al.[32] and Gobble[33, 34] are enthalpies of vaporization $\Delta_{vap}H$.

Compound	*E*	*S*	*A*	*B*	*V*	*L* [1)]	$\Delta_{wiom}H$ (kJ/mol)
DEP [2)]	0.73	1.26	0	0.90	1.7106	6.75	-82.1 [4)]
DnBP [2)]	0.70	1.27	0	0.95	2.2742	8.59	-95.0 [5)]
DiBP [2)]	0.68	1.21	0	0.95	2.2742	8.43	-92.3 [5)]
DPP [2)]	0.68	1.27	0	0.95	2.556	9.63	-106.5 [5)]
BBzP [2)]	1.30	1.51	0	1.13	2.4593	9.95	-106.2 [5)]
DEHP [2)]	0.64	1.25	0	1.02	3.4014	12.70	-116.7 [5)]
DnBA [2)]	0.05	1.12	0	1.03	2.2300	8.14	-83.6 [6)]
DiBA [3)]	0.09	0.92	0	0.97	2.2300	8.04	-80.1 [6)]
DEHA [3)]	0.09	0.92	0	0.97	3.3572	12.16	-114.3 [6)]
DEHTP [3)]	0.75	1.06	0	0.71	3.4014	13.44	-123.3 [5)]
TOTM [3)]	0.81	1.08	0	1.02	4.7493	18.87	-167.1 [6)]
TEHP [3)]	-0.11	0.57	0	0.88	3.9296	13.65	-122.4 [6)]
TPP [2)]	1.83	1.66	0	1.1	2.3714	9.85	-101.2 [6)]

DINCH (low) [3)]	0.11	1.12	0	0.99	3.8122	14.19	-135.7 [6)]
DINCH (high) [3)]	0.11	1.12	0	0.99	3.8122	14.69	-135.7 [6)]

1) Experimental data (see text for details)
2) Experimental descriptors from the UFZ-LSER database[23] (except *L*)
3) Calculated descriptors from the UFZ-LSER database[23] (except *L*)
4) From Rohac et al.[32]
5) From Gobble[33, 34]
6) Calculated from Schwarzenbach et al.[16]

4. Results and Discussion

4.1 Hexadecane/air partitioning coefficients

For the determination of *L*-values, the known data of the calibration compounds DEP, DnBP and DEHP at 298 K were directly correlated with the logarithm of the retention time at 250 °C and 280 °C, respectively. The solutions of the three unknowns in each linear system of equation (14) are as follows: l_L(250 °C) = 0.34972, v_L(250 °C) = -0.83553, c_L(250 °C) = -0.49006; l_L(280 °C) = 0.27344, v_L(280 °C) = -0.72221 and c_L(280 °C) = -0.22469. After inserting the McGowan volume V_i (see Table 1) the unknown *L*-values of the remaining compounds could be calculated. For reasons of quality control, the experiments were performed and two different temperatures, because the calculated *L*-values should be independent of the absolute retention times. As shown in Figure 1, the data for 250 °C and 280 °C are almost identical and the average values of both measurements are presented in Table 1. Additionally, the calculation procedure was checked for both temperatures with DPP, where the experimental *L*-value of 9.55 is known from earlier experiments.[30] DPP was not used as a calibration compound but served for a validation. Its *L*-value could be reproduced with high accuracy (9.55 from Stenzel et al.[30] versus 9.63 from this work). The retention times for the compounds TEHP, DEHTP, DINCH and TOTM were outside the calibration range (DEP → DEHP) and their *L*-values had to be extrapolated. TEHP, DEHTP and DINCH are close to the calibration compound DEHP and the highest uncertainty (18.87 at 250 °C versus 19.13 at 280 °C) was observed for TOTM. This is, however, of minor importance because previous work showed that almost 100% TOTM is expected to be found in the particle phase.[35]

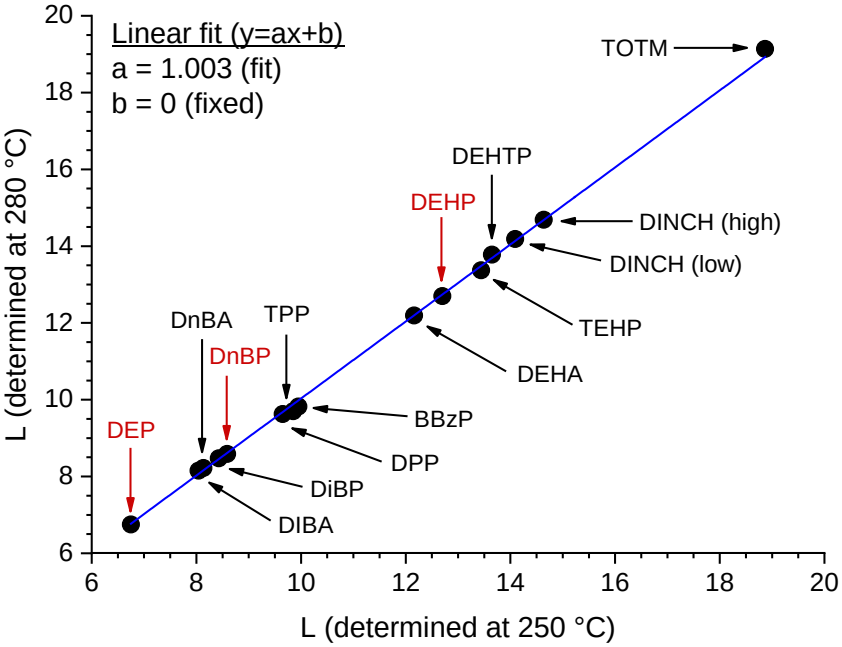

Figure 1: Experimental *L* values as determined at 250 °C and 280 °C by isothermal gas chromatography (see text for details). DEP, DnBP and DEHP (in red) were used as calibration points. DINCH (low) represents the isomer with the lowest retention time and DINCH (high) represents the isomer with the highest retention time.

4.2 Comparison of outdoor and indoor aerosols

The experimental descriptors *s*, *a*, *b*, *l*, *v* and *c* are known for nine different outdoor aerosols at *T* = 288 K and *RH* = 50% from specific historic events (see Supporting Information, Table SI-2) and might not be representative for the for indoor aerosol. The data set provided by Arp et al.[18, 19] covers particle concentrations (PM_{10}) between 8 µg/m³ and 142.2 µg/m³. The fraction of elemental carbon f_{EC} (weight fraction of zero-valent graphitic carbon) was between 0.04 and 0.16 (six aerosols) and the fraction of organic carbon f_{OC} (weight fraction of carbon that can be oxidized to carbon dioxide) was between 0.22 and 0.29 (four aerosols) (see Supporting Information, Table SI-3). These data were compared with aerosol concentrations (Respirable Particulate Matter (RPM), PM_{10} and $PM_{2.5}$) in outdoor and indoor air from several studies.[36-41] The outdoor concentrations (usually 50-P) (P = percentile) were between 12.6 µg/m³ and 78.4 µg/m³. The indoor concentrations (usually 50-P) were between 6.7 µg/m³ and 118.2 µg/m³. There was no trend in the f_{EC} data, all fractions were between 0.04 and 0.14. However, there was a trend towards higher f_{OC} fractions in the indoor aerosols. The maximum was 0.48 but most data were in the range between 0.20 and 0.40. For the outdoor aerosols the range was 0.16 – 0.32. Nevertheless, there is a strong overlap in f_{OC} between

outdoor and indoor aerosols. Several authors published f_{OC} indoor/outdoor ratios with typical values between 0.6 and 1.5.[36, 39] Due to the known heterogeneity of particulate matter, especially in urban environments,[42] it is therefore concluded that the available experimental descriptors from Arp et al.[19] might also represent a good approximation for indoor aerosols. Relevant data from the cited publications are summarized in Table SI-3.

In comparison to ambient particles, the chemical composition of indoor aerosols is often complex, which is due to many specific sources and processes. As outlined by Morawska et al.,[43] the major processes are penetration from outdoors, generation from primary sources (combustion, heating, cooking, electronic devices, household activities), formation of secondary aerosols, deposition and resuspension. The burning of candles for example produces mainly carbonaceous particles,[44] while particles emitted from a laser printer consist of 98% organic compounds.[45]

Apart from organic matter and elemental carbon atmospheric aerosols contain sulfate, nitrate, ammonium, sea salt, mineral dust and water.[46] Wu et al.[47] argue that ammonium sulfate $(NH_4)_2SO_4$ is the main contributor to fine particles derived from secondary aerosol formation in the atmosphere. However, the amount of ammonium and sulfate in the atmospheric aerosol (urban and rural) is usually < 30%.[48] Johnson et al.[41] measured amounts of 11% NH_4^+ and 19% SO_4^{2-} in outdoor generated PM_1, respectively. Under conditions of heavy air pollution, the contribution of ammonium sulfate to the aerosol mass can be about 50%.[49] Rivas et al.[40] found 1% NH_4^+ and 4% SO_4^{2-} in $PM_{2.5}$ of school classrooms. As shown by Goss[50] for polychlorinated hydrocarbons (PCBs), adsorption on inorganic surfaces is small compared to absorption into an organic phase and for an organic matter content of 30% or higher adsorption becomes negligible. Moreover, $(NH_4)_2SO_4$ as a hygroscopic mineral adsorbs large amounts of water and in the range between 20% and 80% its van der Waals surface properties are hardly influenced by the relative humidity.[50]

4.3 Sorption to aerosols

K_{ip}-values (m^3/g) were calculated from equation (6), unit converted to $m^3/\mu g$ and related to 298 K by use of equation (11). The values in Table 2 represent arithmetic mean (AM), standard deviation (STD), median (50-P), minimum and maximum of the individual calculations for the nine aerosols with known descriptors. The range of K_{ip} spans over several orders of magnitude from DEP ($\approx 10^{-6}$ $m^3/\mu g$) to TOTM ($\approx 10^{7}$ $m^3/\mu g$). For the individual compounds the range of K_{ip} (maximum -minimum) is about one order of magnitude with an increasing trend towards molecules with higher molecular weight. Wei et al.[51] derived K_{ip}-data from empirical equations by use of a Monte-Carlo technique. The authors report 50-P values for DEP ($K_{ip} = 4.57 \cdot 10^{-5}$ $m^3/\mu g$), DiBP ($K_{ip} = 2.57 \cdot 10^{-4}$ $m^3/\mu g$), DnBP (K_{ip} =

315 $5.75 \cdot 10^{-4}$ m³/µg), BBzP (K_{ip} = $1.62 \cdot 10^{-3}$ m³/µg) and DEHP (K_{ip} = $3.31 \cdot 10^{-2}$ m³/µg) but, as
316 shown earlier by Salthammer and Schripp,[17] come out with unreasonably broad distributions.

317

318 **Table 2:** K_{ip} values (298 K) as determined from Abraham descriptors (see Table 1) and
319 aerosol descriptors (see Arp et al.[18, 19] and Table SI-2) by use of equations (6) and (11).

Compound	K_{ip} (AM) (m³/µg)	K_{ip} (STD) (m³/µg)	K_{ip} (50-P) (m³/µg)	K_{ip} (min) (m³/µg)	K_{ip} (max) (m³/µg)
DEP	$1.57 \cdot 10^{-6}$	$9.47 \cdot 10^{-7}$	$1.55 \cdot 10^{-6}$	$4.47 \cdot 10^{-7}$	$3.16 \cdot 10^{-6}$
DnBP	$6.17 \cdot 10^{-5}$	$4.92 \cdot 10^{-5}$	$5.39 \cdot 10^{-5}$	$1.63 \cdot 10^{-5}$	$1.74 \cdot 10^{-4}$
DiBP	$4.27 \cdot 10^{-5}$	$3.38 \cdot 10^{-5}$	$3.70 \cdot 10^{-5}$	$1.12 \cdot 10^{-5}$	$1.20 \cdot 10^{-4}$
DPP	$4.37 \cdot 10^{-4}$	$3.97 \cdot 10^{-4}$	$3.50 \cdot 10^{-4}$	$1.11 \cdot 10^{-4}$	$1.38 \cdot 10^{-3}$
BBzP	$1.34 \cdot 10^{-3}$	$1.14 \cdot 10^{-3}$	$1.08 \cdot 10^{-3}$	$2.93 \cdot 10^{-4}$	$3.89 \cdot 10^{-3}$
DEHP	$1.94 \cdot 10^{-1}$	$2.44 \cdot 10^{-1}$	$1.10 \cdot 10^{-1}$	$3.88 \cdot 10^{-2}$	$7.94 \cdot 10^{-1}$
DnBA	$2.37 \cdot 10^{-5}$	$1.74 \cdot 10^{-5}$	$2.02 \cdot 10^{-5}$	$5.92 \cdot 10^{-6}$	$6.19 \cdot 10^{-5}$
DiBA	$1.13 \cdot 10^{-5}$	$7.45 \cdot 10^{-6}$	$9.16 \cdot 10^{-6}$	$9.16 \cdot 10^{-6}$	$2.64 \cdot 10^{-5}$
DEHA	$2.83 \cdot 10^{-2}$	$3.12 \cdot 10^{-2}$	$1.56 \cdot 10^{-2}$	$6.70 \cdot 10^{-3}$	$1.04 \cdot 10^{-1}$
DEHTP	$2.07 \cdot 10^{-1}$	$2.07 \cdot 10^{-1}$	$1.11 \cdot 10^{-1}$	$5.65 \cdot 10^{-2}$	$6.87 \cdot 10^{-1}$
TOTM	$8.09 \cdot 10^{3}$	$1.02 \cdot 10^{4}$	$2.19 \cdot 10^{3}$	$9.53 \cdot 10^{2}$	$3.11 \cdot 10^{4}$
TEHP	$2.41 \cdot 10^{-1}$	$3.02 \cdot 10^{-1}$	$9.78 \cdot 10^{-2}$	$5.69 \cdot 10^{-2}$	$9.87 \cdot 10^{-1}$
TPP	$1.58 \cdot 10^{-3}$	$1.38 \cdot 10^{-3}$	$1.21 \cdot 10^{-3}$	$3.50 \cdot 10^{-4}$	$4.70 \cdot 10^{-3}$
DINCH (low)	$2.03 \cdot 10^{0}$	$2.70 \cdot 10^{0}$	$9.21 \cdot 10^{-1}$	$4.00 \cdot 10^{-1}$	$8.67 \cdot 10^{0}$
DINCH (high)	$4.06 \cdot 10^{0}$	$4.86 \cdot 10^{0}$	$1.84 \cdot 10^{0}$	$8.58 \cdot 10^{-1}$	$1.56 \cdot 10^{1}$

320

321

322 Figure 2 shows a comparison of the K_{ip}-values (arithmetic means (■), minima and maxima
323 (whiskers)) from Table 1 with calculated K_{ip}-values from equation (2). The K_{OA}-values were
324 obtained from SPARC[52] (see Supporting Information). An organic carbon fraction f_{OC} = 0.25
325 was assumed. The fraction of organic matter was then calculated from $f_{OM} = 1.6 \cdot f_{OC} = 0.4$ as
326 proposed by Turpin and Lim.[53] This is in agreement with Weschler and Nazaroff,[1] the value
327 of f_{OM} = 0.2 as proposed by Bidleman and Harner[54] was considered to be unreasonably low.

Moreover, K_{ip}-values for the five phthalates DEP, DiBP, DnBP, BBzP and DEHP from Weschler et al.[55] are presented. These authors used K_{OA}-values from the "three solubility" approach by Cousins and Mackay[51] and applied the equation log K_{ip} = log K_{OA} - 11.72 as derived by Finizio et al.[9] For the determination of K_{ip} from P_s according to equation (1) the approach from Naumova et al.[56] log K_{ip} = -0.860 · log P_s - 4.67 was applied. It is obvious that in most cases the K_{ip} derived from K_{OA} and P_s are significantly higher than K_{ip} from pp-LFER.

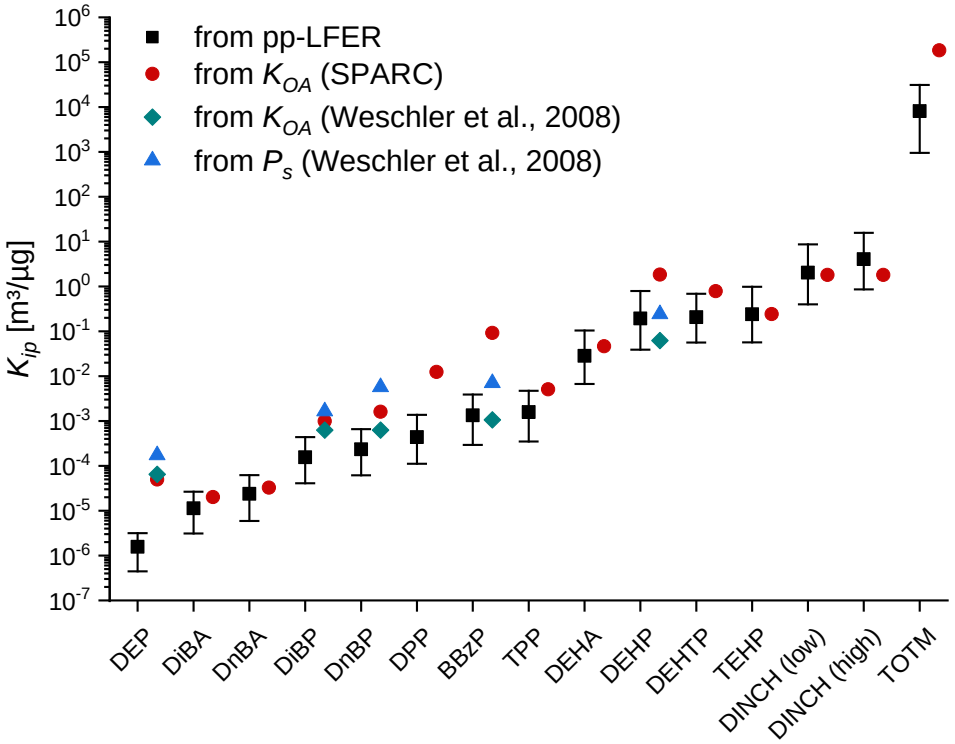

Figure 2: Calculated K_{ip}-values for 298 K from Table 1. The filled squares (■) are the arithmetic mean and the whiskers represent minima and maxima. Calculated K_{ip} from equation (2) using f_{OM} = 0.4 and K_{OA}-values from SPARC (see Table SI-4 in the Supporting Information) are also presented (●). Other K_{ip}-values (♦ and ▲) were taken from Weschler et al.[50]

The need for an estimated K_{OA}-value is a considerable disadvantage of equation (2). This was already investigated by Salthammer and Schripp,[17] who evaluated K_{OA}-data from different sources. Taking DEHP as an example, reported log K_{OA}-values range over more than two orders of magnitude from 10.53 (Cousins and Mackay[57]) to 12.89 (SPARC). Zhang et al.[58] came to analogous results when comparing physical-chemical property estimates for 94 halogenated and organophosphate flame retardants.

The pp-LFER approach (see equation 15) provides values for DEHP of log K_{OA}(dry octanol) = 13.16 and K_{OA}(wet octanol) = 13.02. All data are summarized in the Supporting Information. It is generally obvious that K_{OA}(SPARC) > K_{OA}(pp-LFER) for molecules of low molecular weight and K_{OA}(SPARC) < K_{OA}(pp-LFER) for molecules of high molecular weight. In some cases the deviations are in the order of a magnitude. A similar problem arises if K_{ip} is derived from P_s. As shown by Schossler et al.,[35] K_{ip} being calculated from K_{OA} and P_s can widely differ, which is due to the uncertainties in the descriptors. The pp-LFER approach overcomes this problem by defining different descriptors for van der Waals interactions (*L,* which can be precisely measured) polarizability (*S*) and donor/acceptor interactions (*A, B*). For the compounds being considered here it is a further advantage that the donor term *A* can be neglected.

4.4 Sorption of DEHP to a pure organic phase

Wu et al.[47] studied the distribution of DEHP between air and two different types of organic particles (squalane and oleic acid) at 298 K. For oleic acid, K_{ip} from eight independent measurements ranged from 0.05 m³/µg to 0.41 m³/µg with an arithmetic mean of 0.23 m³/µg. For squalane, K_{ip} from nine independent measurements ranged from 0.04 m³/µg to 0.37 m³/µg with an arithmetic mean of 0.11 m³/µg. This is in good agreement with the K_{ip}-values for DEHP as calculated from the pp-LFER approach at 298 K (see Figure 3). In other words, the gas/particle distribution of DEHP can be equally described by pure organic particles (f_{OM} = 1) and by urban aerosols (f_{OM} ≈ 0.4). This is surprising because K_{ip} is directly proportional to f_{OM} and probably due to the large standard deviations (0.13 m³/µg for oleic acid,[43] 0.10 for squalane[47] and 0.24 m³/µg (see Table 2) for aerosols), which do not allow to distinguish between K_{ip} values within a factor of 2.5.

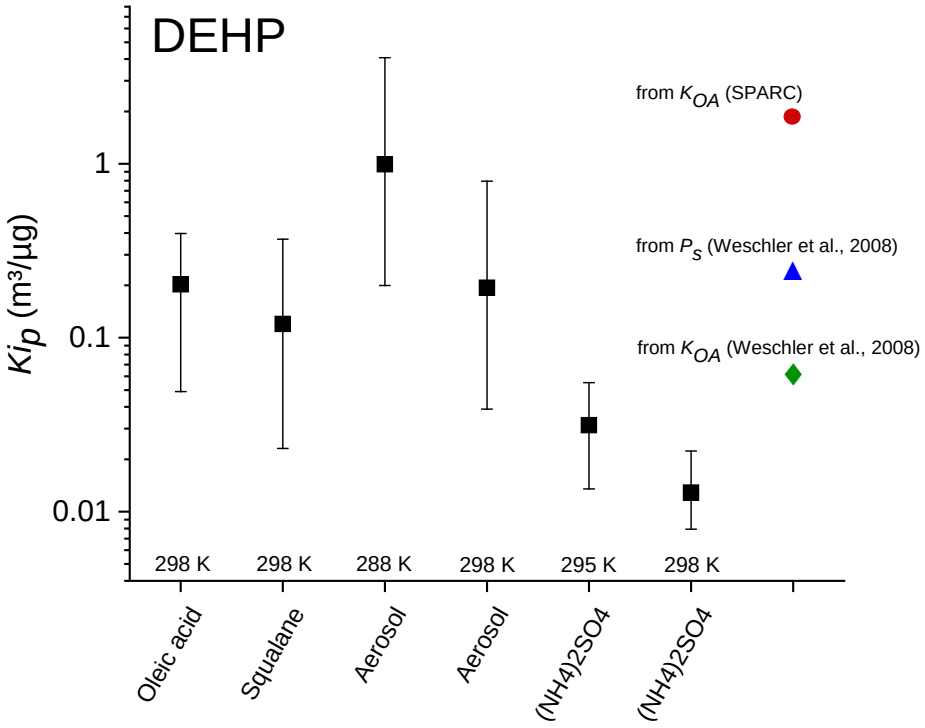

Figure 3: Measured and calculated K_{ip}-values (arithmetic mean (■), minima and maxima) for DEHP. Oleic acid (298 K) and squalane (298 K): Wu et al.;[47] aerosol (288 K) and aerosol (298 K): this work; $(NH_4)_2SO_4$ (298 K): Wu et al.;[47] $(NH_4)_2SO_4$ (295 K): Benning et al.;[59] other data: (●) this work, (♦ and ▲) Weschler et al.[55]

For squalane and oleic acid the ratio c_{part}/c_g, where c_{part} is the total mass of DEHP sorbed to the particle divided by the particle volume and c_g is the gas phase concentration, should be in the range of the octanol/air (K_{OA}) and hexadecane/air (L) distribution coefficient for DEHP. Wu et al.[47] report log (c_{part}/c_g) values of 11.18 for oleic acid and 10.95 for squalane. These values are lower than the calculated data from SPARC (K_{OA} = 12.89) and pp-LFER (K_{OA} = 13.12, L = 12.70). However, it must be kept in mind that K_{OA} is a predicted value and L is a measured value. SPARC also allows the prediction of the squalane/air distribution coefficient K_{SqA} from the squalane/water distribution coefficient and Henry' constant. For DEHP, log K_{SqA} = 12.67, which is in the expected range of log K_{OA} and L. The differences to log (c_{part}/c_g) are higher than an order of magnitude, which might be due to experimental uncertainties. In particular, the calculated particle volume being obtained from a scanning mobility particle sizer (SMPS) is usually error-prone. Especially for the case of a compound with a high log K_{OA} and L value, which means high concentration in the organic phase and low concentration in the gas phase, small changes in c_{part} and c_g cause high deviations of their ratio.

Table 3: Descriptors of various sorbents (solvent/air for octanol and hexadecane; surface/air for $(NH_4)_2SO_4$) as taken from the UFZ-LSER database.[23]

Sorbent	*e*	*s*	*a*	*b*	*v*	*l*	*c*	T (K)
wet octanol [1)]	0.09	0.70	3.48	1.48		0.85	-0.22	298
dry octanol [1)]	-0.21	0.56	3.51	0.75		0.94	-0.15	298
wet + dry hexadecane [1)]						1.00		298
$(NH_4)_2SO_4$ [2)] (20% RH)			2.46	5.23		0.90	-8.47	288
$(NH_4)_2SO_4$ [2)] (40% RH)			2.46	5.23		0.89	-8.47	288
$(NH_4)_2SO_4$ [2)] (60% RH)			2.13	5.34		0.88	-8.47	288

1) Abraham et al.[60]

2) Goss et al.[27]

4.5 Sorption of DEHP to ammonium sulfate

Benning et al.[59] determined K_{ip} for the gas/particle distribution of DEHP between air and ammonium sulfate particles (medium diameter 45 +/- 5 nm) at 295 K. From eight independent measurements K_{ip} ranged from 0.014 m³/µg to 0.55 m³/µg with an arithmetic mean of 0.032 m³/µg. Wu et al.[47] used a similar experimental approach and report a range from 0.008 m³/µg to 0.022 m³/µg with an arithmetic mean of 0.011 m³/µg from 10 independent measurements at 298 K. As shown in Figure 3, the K_{ip}-values for $(NH_4)_2SO_4$ are about an order of magnitude lower than the experimentally determined and calculated K_{ip}-values for aerosols that include organic matter. This can be explained by different sorption mechanisms. Furthermore, Wu et al.[47] discuss the influence of the active area in case of adsorption and conclude that their deviations from the Benning et al.[59] data is due to different size distributions of the $(NH_4)_2SO_4$ particles. Wu et al.[47] also determined $K_{isurf} \approx 300$ m (see equation 7), the particle surface/volume ratio was obtained from particle counting measurements under consideration of the density of $(NH_4)_2SO_4$. This is comparable to the results of previous studies on the adsorption of DEHP on surfaces.[61]

The chamber experiments by Benning et al.[59] were conducted using clean, dry cylinder air for particle generation. Following particle generation, the air stream was passed through a diffusion dryer. Wu et al.[47, 61] do not mention or discuss the relative humidity during their chamber experiments. However, Wu et al.[47] provided the information that the $(NH_4)_2SO_4$

particles were dried and that the humidity in their chamber was almost zero (Yaoxing Wu, personal communication). As comprehensively outlined by Goss,[50] the adsorption at inorganic surfaces is strongly influenced by the relative humidity. If a hygroscopic surface like $(NH_4)_2SO_4$ is covered with water it can be assumed that the water layer is a saturated solution of the salt. The organic molecules interact with this water layer rather than the mineral surface itself. As shown in Table 3, the $(NH_4)_2SO_4$ sorption descriptors are almost identical at RH = 20%, 40% and 60%, respectively. When applying equation (8) for estimating the distribution of DEHP between air and a $(NH_4)_2SO_4$-surface at 288 K, the results are log K_{isurf}(288 K, 20% RH) = 8.32 m, log K_{isurf}(288 K, 40% RH) = 8.18 m and log K_{isurf}(288 K, 60% RH) = 8.15 m. The enthalpy of adsorption $\Delta_{surf}H_i$, calculated from equation (12), is ≈ 170 kJ/mol, which leads to log K_{isurf}(298 K) values in the range of 7.2 (see equation 13). These coefficients are considerably higher than the reported log K_{isurf} = log 300 (m) ≈ 2.5 by Wu et al.[47]

This discrepancy cannot easily be resolved. However, we do not feel the need for a comprehensive discussion of SVOC adsorption on dry or wet $(NH_4)_2SO_4$ surfaces, because this type of aerosol is not of importance for the indoor environment. Seinfeld and Pandis[62] showed that neither ammonia nor sulfate dominate the chemical composition of urban, rural, remote, desert and maritime aerosols. The same authors demonstrate the high complexity of ammonia-sulfate-water chemistry of atmospheric aerosols. Storey et al.[63] point out that gas/solid partitioning coefficients, which are significantly below the coefficients for urban particulate matter, hardly play a role in environmental processes. Finally, the determination of K_{isurf} values is often subject to error, because the calculation of particle surface areas from SMPS data is associated with some uncertainties.[64]

4.6 Fraction in gas phase and particle phase

For exposure analysis it is of considerable importance to know if the compound of interest *i* is primarily in the gas phase or particle-bound.[65] This information can be obtained from equation (4) under assumption of equilibrium conditions. When considering particle diameters < 1 µm, the time to achieve equilibrium is less than 1min for compounds with a K_{OA} < 10.5 and 1 min – 1 h for compounds with K_{OA} > 10.5.[1] Figure 4 shows scenarios for TSP-concentrations of 10 µg/m³, 25 µg/m³ and 50 µg/m³, respectively. The K_{ip}-values are the arithmetic means from Table 1. It becomes obvious that DEP, DiBA, DnBA, DiBP and DnBP are expected to be found in the gas phase. It is also clear that for DINCH and TOTM more than 90% are expected in the particle phase. The overall quality of the descriptors is of minor importance for the results of DINCH and TOTM, which is due to the high K_{OA}- and *L*-values. However, more difficult situations arise for the other SVOCs. It is obvious that the major

fractions of DEHP, DEHTP and TEHP will be found in the particle phase (> 80% for *[TSP]* > 25 µg/m³). For DEHP, this is in accordance with the study by Salthammer and Schripp,[17] who calculated a particle-bound fraction higher than 75%. For DPP and BBzP, the K_{ip} from K_{OA}(SPARC) is significantly higher than K_{ip} from pp-LFER. The situation is similar for TPP but the deviation is smaller. Consequently, the pp-LFER approach predicts a fraction of more than 90% DPP, BBzP and TPP in the gas phase. Especially in case of BBzP, K_{ip} from equation (2) allows for higher particle-bound fractions, which is due to the K_{OA}(SPARC) of 11.59. For DEHA the K_{ip} from pp-LFER is $2.83 \cdot 10^{-2}$ m³/µg. This means that even small changes of the TSP-concentration cause high changes of the particle-bound fraction, which makes a prediction very uncertain. Sühring et al.[66] studied the gas/particle partitioning of several organic esters and come to analogous results for TPP and TEHP on the basis of single-parameter models. Okeme et al.[67] compared experimental gas/particle partitioning data of organophosphate esters with single- and pp-models and state that for this class of compounds the sampling on filters might be subject to artifacts.

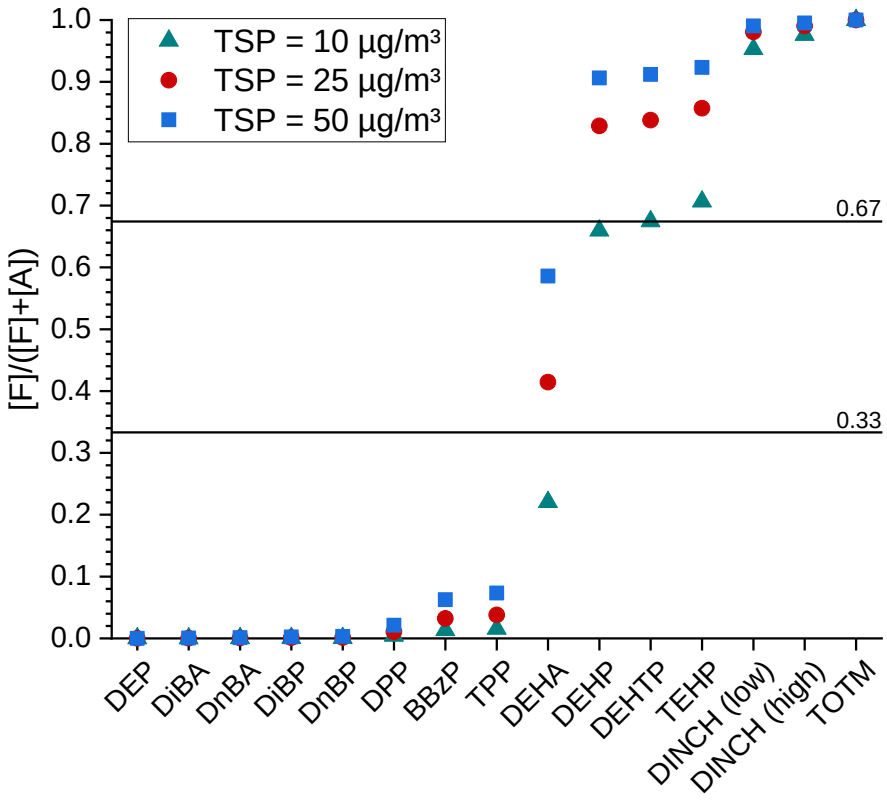

Figure 4: Particle-bound fractions Φ of the 14 SVOCs for different concentrations of TSP. The fractions were calculated by use of equation (4) and the K_{ip}-values are the arithmetic means from Table 1. Please not that DINCH (low) and DINCH (high) refer to different isomers (see text for details).

The pp-LFER approach appears as an advanced tool for the prediction of gas/particle distributions of SVOCs. However, when taking into account uncertainties of the experimentally determined and calculated predictors as well as the heterogeneity of aerosols, it seems to be unlikely that precise estimates of K_{ip} can be made. As already discussed,[17] such predictions yield quite reliable results for compounds of very high and very low volatility. However, for compounds with a K_{ip} in the range of 10^{-1} - 10^{-2} m³/µg equation (4) causes high uncertainties. The aerosol descriptors available from Arp et al.[19] appear applicable for the indoor environment. Nevertheless, it would be beneficial to determine aerosol descriptors from a data set of true indoor aerosols.

Acknowledgements

The authors are grateful to Prof. John C. Little and his co-workers, especially Yaoxing Wu, for providing the raw data of their study Wu et al. (2018) Environ. Sci. Technol. 52, 3583-3590 and to Alexander Omelan (WKI) for his analytical support. This work was financially supported by internal Fraunhofer WKI research funds. Graphical Abstract design: Klara Salthammer.

References

1. Weschler, C. J.; Nazaroff, W. W., Semivolatile organic compounds in indoor environments. *Atmospheric Environment* **2008,** *42*, (40), 9018-9040.
2. Weschler, C. J.; Nazaroff, W. W., SVOC partitioning between the gas phase and settled dust indoors. *Atmospheric Environment* **2010,** *44*, (30), 3609-3620.
3. Liang, Y.; Bi, C.; Wang, X.; Xu, Y., A general mechanistic model for predicting the fate and transport of phthalates in indoor environments. *Indoor Air* **2019,** *29*, (1), 55-69.
4. Ott, W. R.; Steinemann, A. C.; Wallace, L. A., *Exposure Analysis*. CRC Press: Boca Raton, 2007.
5. Junge, C. E., Transport mechanisms for pesticides in the atmosphere. *Pure & Applied Chemistry* **1975,** *42*, 95-104.
6. Junge, C. E., Basic considerations about trace constituents in the atmosphere as related to the fate of global pollutants. In *Fate of Pollutants in the Air and Water Environments, Part I*, Suffet, I. H., Ed. John Wiley & Sons: New York, 1977; pp 7-25.
7. Pankow, J. F., Review and comparative analysis of the theories on partitioning between the gas and aerosol particulate phases in the atmosphere. *Atmospheric Environment* **1987,** *21*, 2275–2283.
8. Pankow, J. F., An absorption model of gas/particle partitioning of organic compounds in the atmosphere. *Atmospheric Environment* **1994,** *28*, (2), 185-188.
9. Finizio, A.; Mackay, D.; Bidleman, T.; Harner, T., Octanol-air partition coefficient as a predictor of partitioning of semi-volatile organic chemicals to aerosols. *Atmospheric Environment* **1997,** *31*, (15), 2289-2296.
10. Yamasaki, H.; Kuwata, K.; Miyamoto, H., Effects of ambient temperature on aspects of airborne polycyclic aromatic hydrocarbons. *Environmental Science & Technology* **1982,** *16*, (4), 189-194.
11. Pankow, J. F., Further discussion of the octanol/air partition coefficient Koa as a correlating parameter for gas/particle partitioning coefficients. *Atmospheric Environment* **1998,** *32*, (9), 1493-1497.
12. Goss, K.-U.; Schwarzenbach, R. P., Gas/Solid and Gas/Liquid Partitioning of Organic Compounds: Critical Evaluation of the Interpretation of Equilibrium Constants. *Environmental Science & Technology* **1998,** *32*, (14), 2025-2032.
13. Klöpffer, W., *Verhalten und Abbau von Umweltchemikalien: Physikalisch-chemische Grundlagen* WILEY-VCH: Weinheim, 2012.
14. Goss, K.-U.; Schwarzenbach, R. P., Linear Free Energy Relationships Used To Evaluate Equilibrium Partitioning of Organic Compounds. *Environmental Science & Technology* **2001,** *35*, (1), 1-9.
15. Abraham, M. H., Scales of solute hydrogen-bonding: their construction and application to physicochemical and biochemical processes. *Chemical Society Reviews* **1993,** *22*, (2), 73-83.
16. Schwarzenbach, R. P.; Gschwend, P. M.; Imboden, D. M., *Environmental Organic Chemistry*. John Wiley & Sons: Hoboken, NJ, 2017.
17. Salthammer, T.; Schripp, T., Application of the Junge- and Pankow-equation for estimating indoor gas/particle distribution and exposure to SVOCs. *Atmospheric Environment* **2015,** *106*, (0), 467-476.
18. Arp, H. P. H.; Schwarzenbach, R. P.; Goss, K.-U., Ambient Gas/Particle Partitioning. 2: The Influence of Particle Source and Temperature on Sorption to Dry Terrestrial Aerosols. *Environmental Science & Technology* **2008,** *42*, (16), 5951-5957.
19. Arp, H. P. H.; Schwarzenbach, R. P.; Goss, K.-U., Ambient Gas/Particle Partitioning. 1. Sorption Mechanisms of Apolar, Polar, and Ionizable Organic Compounds. *Environmental Science & Technology* **2008,** *42*, (15), 5541-5547.
20. Goss, K.-U., Predicting the equilibrium partitioning of organic compounds using just one linear solvation energy relationship (LSER). *Fluid Phase Equilibria* **2005,** *233*, (1), 19-22.
21. Abraham, M. H.; McGowan, J. C., The use of characteristic volumes to measure cavity terms in reversed phase liquid chromatography. *Chromatographia* **1987,** *23*, (4), 243-246.

22. Abraham, M. H.; Whiting, G. S.; Doherty, R. M.; Shuely, W. J., Hydrogen bonding. Part 13. A new method for the characterisation of GLC stationary phases - The Laffort data set. *Journal of the Chemical Society, Perkin Transactions 2* **1990**, (8), 1451-1460.
23. Ulrich, N.; Endo, S.; Brown, T. N.; Watanabe, N.; Bronner, G.; Abraham, M. H.; Goss, K.-U., UFZ-LSER database v 3.2.1 [Internet]. In Helmholtz Centre for Environmental Research: Leipzig, 2017.
24. Weininger, D., SMILES, a chemical language and information system. 1. Introduction to methodology and encoding rules. *Journal of Chemical Information and Computer Sciences* **1988,** *28*, (1), 31-36.
25. Brown, T. N.; Arnot, J. A.; Wania, F., Iterative fragment selection: A group contribution approach to predicting fish biotransformation half-lives. *Environmental Science and Technology* **2012,** *46*, (15), 8253-8260.
26. Brown, T. N., Predicting hexadecane-air equilibrium partition coefficients (L) using a group contribution approach constructed from high quality data. *SAR and QSAR in Environmental Research* **2014,** *25*, (1), 51-71.
27. Goss, K. U.; Buschmann, J.; Schwarzenbach, R. P., Determination of the surface sorption properties of talc, different salts, and clay minerals at various relative humidities using adsorption data of a diverse set of organic vapors. *Environmental Toxicology and Chemistry* **2003,** *22*, (11), 2667-2672.
28. Goss, K.-U.; Schwarzenbach, R. P., Empirical Prediction of Heats of Vaporization and Heats of Adsorption of Organic Compounds. *Environmental Science & Technology* **1999,** *33*, (19), 3390-3393.
29. Arp, H. P. H.; Goss, K.-U.; Schwarzenbach, R. P., Evaluation of a predictive model for air/surface adsorption equilibrium constants and enthalpies. *Environmental Toxicology and Chemistry* **2006,** *25*, (1), 45-51.
30. Stenzel, A.; Endo, S.; Goss, K.-U., Measurements and predictions of hexadecane/air partition coefficients for 387 environmentally relevant compounds. *Journal of Chromatography A* **2012,** *1220*, 132-142.
31. Abraham, M. H.; Acree, W. E., Physicochemical and biochemical properties for the dialkyl phthalates. *Chemosphere* **2015,** *119*, 871-880.
32. Roháč, V.; Růžička, K.; Růžička, V.; Zaitsau, D. H.; Kabo, G. J.; Diky, V.; Aim, K., Vapour pressure of diethyl phthalate. *The Journal of Chemical Thermodynamics* **2004,** *36*, (11), 929-937.
33. Gobble, C.; Chickos, J.; Verevkin, S. P., Vapor pressures and vaporization enthalpies of a series of dialkyl phthalates by correlation gas chromatography. *Journal of Chemical and Engineering Data* **2014,** *59*, (4), 1353-1365.
34. Gobble, C. P. Study of Vaporization Enthalpies and Vapor Pressures of Potential Environmental Pollutants by Correlation-Gas Chromatography. University of Missouri, St. Louis, 2016.
35. Schossler, P.; Schripp, T.; Salthammer, T.; Bahadir, M., Beyond phthalates: Gas phase concentrations and modeled gas/particle distribution of modern plasticizers. *Science of the Total Environment* **2011,** *409*, 4031-4038.
36. Ho, K. F.; Cao, J. J.; Harrison, R. M.; Lee, S. C.; Bau, K. K., Indoor/outdoor relationships of organic carbon (OC) and elemental carbon (EC) in PM2.5 in roadside environment of Hong Kong. *Atmospheric Environment* **2004,** *38*, (37), 6327-6335.
37. Long, C. M.; Suh, H. H.; Koutrakis, P., Characterization of indoor particle sources using continuous mass and size monitors. *Journal of the Air and Waste Management Association* **2000,** *50*, (7), 1236-1250.
38. Fromme, H.; Lahrz, T.; Hainsch, A.; Oddoy, A.; Piloty, M.; Rüden, H., Elemental carbon and respirable particulate matter in the indoor air of apartments and nursery schools and ambient air in Berlin (Germany). *Indoor Air* **2005,** *15*, (5), 335-341.
39. Fromme, H.; Diemer, J.; Dietrich, S.; Cyrys, J.; Heinrich, J.; Lang, W.; Kiranoglu, M.; Twardella, D., Chemical and morphological properties of particulate matter (PM10, PM2.5) in school classrooms and outdoor air. *Atmospheric Environment* **2008,** *42*, (27), 6597-6605.

40. Rivas, I.; Viana, M.; Moreno, T.; Pandolfi, M.; Amato, F.; Reche, C.; Bouso, L.; Alvarez-Pedrerol, M.; Alastuey, A.; Sunyer, J.; Querol, X., Child exposure to indoor and outdoor air pollutants in schools in Barcelona, Spain. *Environment International* **2014,** *69*, 200-212.
41. Johnson, A. M.; Waring, M. S.; DeCarlo, P. F., Real-time transformation of outdoor aerosol components upon transport indoors measured with aerosol mass spectrometry. *Indoor Air* **2017,** *27*, (1), 230-240.
42. Lazaridis, M., Organic Aerosols. In *Environmental Chemistry of Aerosols*, Colbeck, I., Ed. Blackwell Publishing Ltd.: Oxford, 2008; pp 91-115.
43. Morawska, L.; Afshari, A.; Bae, G. N.; Buonanno, G.; Chao, C. Y. H.; Hänninen, O.; Hofmann, W.; Isaxon, C.; Jayaratne, E. R.; Pasanen, P.; Salthammer, T.; Waring, M.; Wierzbicka, A., Indoor aerosols: from personal exposure to risk assessment. *Indoor Air* **2013,** *23*, (6), 462-487.
44. Stabile, L.; Fuoco, F. C.; Buonanno, G., Characteristics of particles and black carbon emitted by combustion of incenses, candles and anti-mosquito products. *Building and Environment* **2012,** *56*, 184-191.
45. Morawska, L.; He, C.; Johnson, G.; Jayaratne, R.; Salthammer, T.; Wang, H.; Uhde, E.; Bostrom, T.; Modini, R.; Ayoko, G.; McGarry, P.; Wensing, M., An Investigation into the Characteristics and Formation Mechanisms of Particles Originating from the Operation of Laser Printers. *Environmental Science & Technology* **2009,** *43*, (4), 1015-1022.
46. Pöschl, U., Atmospheric Aerosols: Composition, Transformation, Climate and Health Effects. *Angewandte Chemie International Edition* **2005,** *44*, (46), 7520-7540.
47. Wu, Y.; Eichler, C. M. A.; Cao, J.; Benning, J.; Olson, A.; Chen, S.; Liu, C.; Vejerano, E. P.; Marr, L. C.; Little, J. C., Particle/Gas Partitioning of Phthalates to Organic and Inorganic Airborne Particles in the Indoor Environment. *Environmental Science and Technology* **2018,** *52*, (6), 3583-3590.
48. Putaud, J. P.; Van Dingenen, R.; Alastuey, A.; Bauer, H.; Birmili, W.; Cyrys, J.; Flentje, H.; Fuzzi, S.; Gehrig, R.; Hansson, H. C.; Harrison, R. M.; Herrmann, H.; Hitzenberger, R.; Hüglin, C.; Jones, A. M.; Kasper-Giebl, A.; Kiss, G.; Kousa, A.; Kuhlbusch, T. A. J.; Löschau, G.; Maenhaut, W.; Molnar, A.; Moreno, T.; Pekkanen, J.; Perrino, C.; Pitz, M.; Puxbaum, H.; Querol, X.; Rodriguez, S.; Salma, I.; Schwarz, J.; Smolik, J.; Schneider, J.; Spindler, G.; ten Brink, H.; Tursic, J.; Viana, M.; Wiedensohler, A.; Raes, F., A European aerosol phenomenology – 3: Physical and chemical characteristics of particulate matter from 60 rural, urban, and kerbside sites across Europe. *Atmospheric Environment* **2010,** *44*, (10), 1308-1320.
49. Chan, C. K.; Yao, X., Air pollution in mega cities in China. *Atmospheric Environment* **2008,** *42*, (1), 1-42.
50. Goss, K.-U., The Air/Surface Adsorption Equilibrium of Organic Compounds Under Ambient Conditions. *Critical Reviews in Environmental Science and Technology* **2004,** *34*, (4), 339-389.
51. Wei, W.; Mandin, C.; Blanchard, O.; Mercier, F.; Pelletier, M.; Le Bot, B.; Glorennec, P.; Ramalho, O., Distributions of the particle/gas and dust/gas partition coefficients for seventy-two semi-volatile organic compounds in indoor environment. *Chemosphere* **2016,** *153*, 212-219.
52. Hilal, S. H.; Karickhoff, S. W.; Carreira, L. A., Prediction of the vapor pressure boiling point, heat of vaporization and diffusion coefficient of organic compounds. *Qsar & Combinatorial Science* **2003,** *22*, (6), 565-574.
53. Turpin, B. J.; Lim, H.-J., Species Contributions to PM2.5 Mass Concentrations: Revisiting Common Assumptions for Estimating Organic Mass. *Aerosol Science and Technology* **2001,** *35*, (1), 602 - 610.
54. Bidleman, T. F.; Harner, T., Sorption to Aerosols. In *Handbook of property Estimation Methods for Chemicals*, Boethling, R. S.; Mackay, D., Eds. Lewis Publishers: Boca Raton, 2000; pp 233-260.
55. Weschler, C. J.; Salthammer, T.; Fromme, H., Partitioning of phthalates among the gas phase, airborne particles and settled dust in indoor environments. *Atmospheric Environment* **2008,** *42*, (7), 1449-1460.
56. Naumova, Y. Y.; Offenberg, J. H.; Eisenreich, S. J.; Meng, Q.; Polidori, A.; Turpin, B. J.; Weisel, C. P.; Morandi, M. T.; Colome, S. D.; Stock, T. H.; Winer, A. M.; Alimokhtari, S.; Kwon, J.; Maberti, S.;

Shendell, D.; Jones, J.; Farrar, C., Gas/particle distribution of polycyclic aromatic hydrocarbons in coupled outdoor/indoor atmospheres. *Atmospheric Environment* **2003,** *37*, (5), 703-719.
57. Cousins, I.; Mackay, D., Correlating the physical-chemical properties of phthalate esters using the 'three solubility' approach. *Chemosphere* **2000,** *41*, (9), 1389-1399.
58. Zhang, X.; Sühring, R.; Serodio, D.; Bonnell, M.; Sundin, N.; Diamond, M. L., Novel flame retardants: Estimating the physical-chemical properties and environmental fate of 94 halogenated and organophosphate PBDE replacements. *Chemosphere* **2016,** *144*, 2401-2407.
59. Benning, J. L.; Liu, Z.; Tiwari, A.; Little, J. C.; Marr, L. C., Characterizing Gas-Particle Interactions of Phthalate Plasticizer Emitted from Vinyl Flooring. *Environmental Science & Technology* **2013,** *47*, (6), 2696-2703.
60. Abraham, M. H.; Smith, R. E.; Luchtefeld, R.; Boorem, A. J.; Luo, R.; Acree, W. E., Jr., Prediction of Solubility of Drugs and Other Compounds in Organic Solvents. *Journal of Pharmaceutical Sciences* **2010,** *99*, (3), 1500-1515.
61. Wu, Y.; Eichler, C. M. A.; Leng, W.; Cox, S. S.; Marr, L. C.; Little, J. C., Adsorption of Phthalates on Impervious Indoor Surfaces. *Environmental Science & Technology* **2017,** *51*, (5), 2907-2913.
62. Seinfeld, J. H.; Pandis, S. N., *Atmospheric Chemistry and Physics*. John Wiley & Sons: New York, 2016.
63. Storey, J. M. E.; Luo, W.; Isabelle, L. M.; Pankow, J. F., Gas/Solid Partitioning of Semivolatile Organic Compounds to Model Atmospheric Solid Surfaces as a Function of Relative Humidity. 1. Clean Quartz. *Environmental Science and Technology* **1995,** *29*, (9), 2420-2428.
64. Baron, P. A.; Willeke, K., *Aerosol Measurement. Principles, Techniques, and Applications* John Wiley & Sons: New York, 2005.
65. Salthammer, T.; Zhang, Y.; Mo, J.; Koch, H. M.; Weschler, C. J., Assessing Human Exposure to Organic Pollutants in the Indoor Environment. *Angewandte Chemie International Edition* **2018,** *57*, (38), 12228-12263.
66. Sühring, R.; Wolschke, H.; Diamond, M. L.; Jantunen, L. M.; Scheringer, M., Distribution of Organophosphate Esters between the Gas and Particle Phase-Model Predictions vs Measured Data. *Environmental Science and Technology* **2016,** *50*, (13), 6644-6651.
67. Okeme, J. O.; Rodgers, T. F. M.; Jantunen, L. M.; Diamond, M. L., Examining the Gas-Particle Partitioning of Organophosphate Esters: How Reliable Are Air Measurements? *Environmental Science and Technology* **2018,** *52*, (23), 13834-13844.